Int J Clin Exp Med 2014;7(5):1204-1213
www.ijcem.com /ISSN:1940-5901/IJCEM0000256

Original Article

Evaluation of vesicular stomatitis virus mutant as an oncolytic agent against prostate cancer

Xin Zhao, Shengsong Huang, Huarong Luo, Xiaodong Wan, Yaping Gui, Junliang Li, Denglong Wu

Department of Urology, Tongji Hospital of Tongji University, Shanghai, China

Received March 17, 2014; Accepted May 12, 2014; Epub May 15, 2014; Published May 30, 2014

Abstract: Background: To date, limited options are available to treat malignant prostate cancer, and novel strategies need to be developed. Oncolytic viruses (OV) that have preferential replication capabilities in cancer cells rather than normal cells represent one promising alternative for treating malignant tumors. Vesicular stomatitis virus (VSV) is a non-segmented, negative-strand RNA virus with the inherent capability to selectively kill tumor cells. The aim of this study was to evaluate the potential of VSV-ΔM51-GFP as an effective therapeutic agent for treating prostate tumors. Methods: For in vitro experiments, DU145 and PC3 cell lines were treated with VSV-ΔM51-GFP. Viral titers were quantified using plaque assays. Cytotoxicity was performed by MTT analysis. IFN-β production was measured using a Human IFN-β detection ELISA Kit. The detection of apoptosis was performed via Annexin-V-FITC staining method and analyzed with flow cytometry. The in vivo antitumor efficacy of VSV-ΔM51-GFP in a xenograft mice prostate tumor model. Results: It was observed that VSV-ΔM51-GFP can efficiently replicate and lyse human prostate cancer cells and that this virus has reduced toxicity against normal human prostate epithelial cells in vitro. VSV-ΔM51-GFP in the induction of apoptosis in DU145 cells and PC3 cells. Furthermore, in a xenograft tumor animal model, nude mice bearing replication-competent VSV-ΔM51-GFP were able to eradicate malignant cells while leaving normal tissue relatively unaffected. The survival of the tumor-burdened animals treated with VSV-ΔM51-GFP may also be significantly prolonged compared to mock-infected animals. Conclusions: VSV-ΔM51-GFP showed promising oncolytic activity for treating prostate cancer.

Keywords: Vesicular stomatitis virus, prostate cancer, oncolytic virotherapy

Introduction

Prostate cancer is the most prevalent malignancy and the second leading cause of cancer-related mortality in North American men, with more than 186,000 new cases diagnosed and approximately 28,000 deaths annually [1]. To date, the treatment options for prostate cancer include surgery with radical prostatectomy, hormone therapy, chemotherapy [2] and radiation [3]. There are currently no curative treatment options for patients with locally advanced or metastatic disease [4-6]; therefore, effective new treatment strategies need to be developed.

Oncolytic viruses such as measles virus, reoviruses, and newcastle disease virus are promising alternatives in tumor treatment. Some of these viruses are undergoing clinical trials. The family member vesicular stomatitis virus (VSV) is a small, enveloped, negative-sense single-stranded RNA virus that can selectively replicate in IFN pathway-defective tumor cells, but is strongly suppressed in IFN response-normal tissues. Its rapid and productive replication cycle and wide tropisms grant VSV a strong oncolytic potency. Based on these advantages, VSV has been developed as an oncolytic agent for treating cancers.

VSV has demonstrated preclinical success against a variety of malignancies, including breast cancer [7], melanoma [8, 9], colorectal cancer [10, 11], liver cancer [12-15], glioblastoma [16] and other cancers [17]. Importantly, the oncolytic potential of VSV did not seem to be restricted to tumor cells with specific genetic aberrancies. For example, VSV was able to destroy cells carrying defective Myc or p53 and cells with activated Ras. Wollmann and colleagues have recently compared VSV to eight

other oncolytic viruses [18]. The virus could be safely cleared from normal cells while maintaining its ability to destroy malignant cells, thereby making VSV more cancer specific [8, 9, 15]. VSV showed excellent infectivity, high rates of replication, and strong cytolytic action. While VSV is not considered a significant human pathogen, it can cause neurotoxicity in mice, nonhuman primates, and even humans [18]. However, several VSV mutants have been generated that are not neurotropic but retain their oncolytic activity [19-21]. In this study, we focused on one VSV mutant, VSV-ΔM51-GFP. VSV-ΔM51-GFP has a deletion at amino acid position 51 of the matrix (M) protein, as well as the GFP ORF inserted in position 5 of the viral genome [21].

The goal of this study was to evaluate the oncolytic capability of VSV-ΔM51-GFP against prostate tumors in vitro and in vivo. Our results indicate that this virus is able to selectively infect and replicate in malignant tissue while sparing normal tissue due to a faulty IFN response. Our in vitro and in vivo results demonstrate that VSV-ΔM51-GFP has good potential as an OV against prostate cancer.

Materials and methods

Cells and animals

The normal human prostate epithelial cell line RWPE-1 and human prostate cancer cell line Du145 and PC3 were purchased from the Culture Collection of the Chinese Academy of Sciences, Shanghai, China. DU145 cells and PC3 cells were maintained in RPMI-1640 medium (HyClone, USA) supplemented with 10% fetal bovine serum (HyClone). RWPE-1 cells were maintained in keratinocyte serum-free medium (Invitrogen, USA) supplemented with bovine pituitary extract and recombinant human epidermal growth factor. Vero cells were maintained in RPMI1640 supplemented with 10% fetal bovine serum and 100 units/mL penicillin/streptomycin.

Six-to-eight-week-old male nude mice were purchased from the Shanghai SLAC Experimental Animal Company (Chinese Academy of Sciences, China). The animals were housed in a sterile animal facility with food and water ad libitum. All procedures were reviewed and approved by the University of Tongji Animal Care Committee.

Viral replication and plaque assay quantification

Recombinant VSV encoding green fluorescent protein (GFP) was propagated in Vero cells. Viral titers were quantified using plaque assays. Briefly, 90% confluent Vero cells in 12-well plates were infected with optimally diluted VSV-ΔM51-GFP and then covered with low melting temperature agar (Invitrogen, USA) after rinsing with phosphate buffered saline (PBS). At 24 h post infection (p.i.), 1% crystal violet was used to stain the Vero cells and plaques were quantified.

Cytotoxicity assays

DU145 cells and PC3 cells were seeded in 96-well plates, cultured for 24 h with 80% confluence, and then infected with virus at a multiplicity of infection (MOI) of either 0.1 or 0.01. Mock infections were set up using RPMI-1640 media. One hour post infection, the virus was aspirated and the cells were incubated in growth medium containing 10% FBS. The 3-(4, 5-dimethylthiazol-2-yl)-2,5-diphenyltetrazolium bromide (MTT) assay was used to evaluate cell death. After incubation for 4 h at 37°C, the media and MTT were gently aspirated, and 150 μL of DMSO was added to each well and mixed thoroughly. The absorbance was read at 570 nm with a microplate reader. The cell growth inhibition rate was calculated as follows: cell growth inhibition rate = 1-A_{570} mean value of transduced cells/A_{570} mean value of untransduced cells × 100%.

Type I IFN ELISA

Du145, PC3, RWPE-1 cells were infected with VSV-ΔM51-GFP at a MOI of 0.1. The supernatants were collected from the infected cells 12 and 24 h after infection, and IFN-β production was measured using a Human IFN-β detection ELISA Kit (R&D Company; USA), Following the manufacturer's instructions. Briefly, 50 μl of assay diluent was dispensed to each well, and 100 μl of a standard control sample was added as appropriate. The contents were incubated at room temperature for 2 hours, washed three times with washing buffer, and mixed with 100 μl of diluted antibody solution per well. After a further incubation for 1 hour at room temperature, the plate was washed and 100 μl of diluted HRP solution was dispensed to each well.

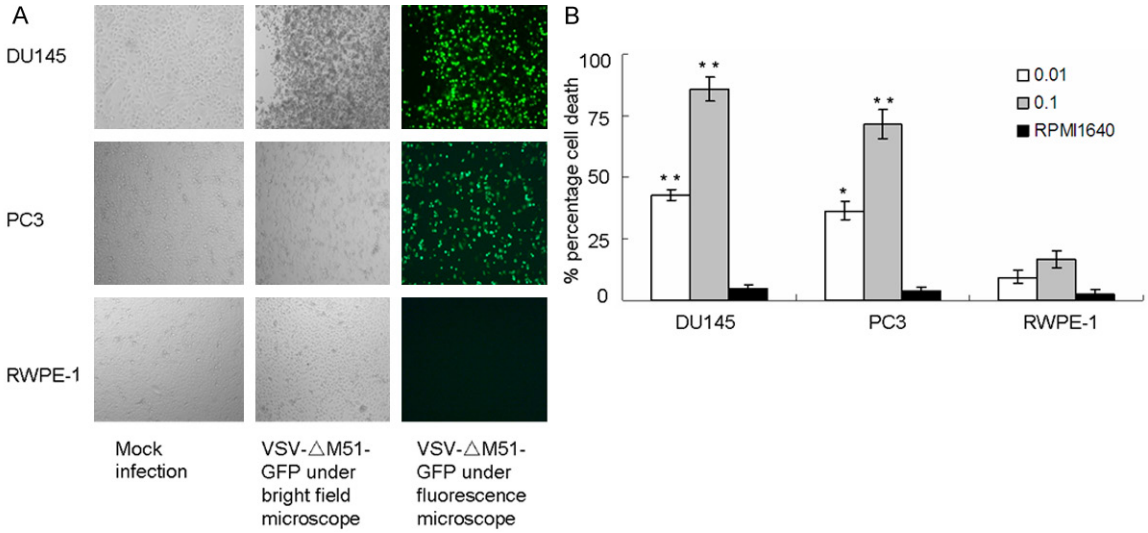

Figure 1. A: Infection of DU145 cells; PC3 cells and RWPE-1 cells with VSV-ΔM51-GFP. DU145 cells PC3 cells were infected with VSV-ΔM51-GFP at MOI of 0.1. Forty-eight hours after inoculation, CPEs could be found in all of the DU145 cells and PC3 with GFP fluorescence also detected. RWPE-1 cells were infected with VSV-ΔM51-GFP at MOI of 0.1. Forty-eight hours after infection, CPEs and GFP fluorescence were detected; few CPEs were detected in mock infection cells. B: Cytotoxicity studies of VSV-ΔM51-GFP in DU145 cells; PC3 cells and RWPE-1 cells. (The symbol *represents $P < 0.05$ compared with RWPE-1, the symbol **represents $P < 0.01$ compared with RWPE-1).

The plate was then washed three times with washing buffer, and 100 μl of TMB Substrate Solution was added to each well; after a 15-minute incubation with TMB, 100 μl of stop solution add was added to each well, and the plates were read on a microplate reader at a primary wavelength of 450 nm.

Flow cytometric analysis of apoptosis and cell death

Annexin-V and PI double staining methods were applied to quantitative apoptosis. The results were analyzed using flow cytometry according to the manufacture's specifications, Briefly, cells were treated with different MOI (0.01 and 0.1) of VSV-ΔM51-GFP and after indicated time, infected and non-infected cells were harvested at the density of 6×10^5 cell/ml, the collected cell were then washed twice by cold PBS, and the cell pallets were then re-suspended in 500 ul of 1X binding buffer. Resuspended cells were undergone gentle vortex and stained with 5 ul of Annexin-V-FITC and 5 ul of PI. Following short incubation for 10 min in the dark at room temperature, the florescence of cells were analyzed by FAC-SCalibur flow cytometer (Becton Dickinson, San Jose, USA) using the ibuiltin software (BD Cell Quest software).

Antitumor activity of VSV-ΔM51-GFP in a xenograft mice prostate tumor model

DU145 cells growing in exponential phase were harvested, washed, and resuspended in RPMI-1640 at a density of 2×10^7 cells/ml. Nude mice were injected in the flanks with 2.0×10^6 cells suspended in 100 μl of RPMI-1640. After two weeks, mice with palpable tumors measuring 1.0 cm^2 were divided into three groups (n = 10 for each group) and received a single intratumoral injection of VSV-ΔM51-GFP at a dose of 1×10^7 pfu or 1×10^6 pfu in 100 μl volume. A group of tumor-bearing animals was injected with RPMI-1640 as a negative control. The tumor sizes were measured and recorded every five days. The tumor-bearing mice were sacrificed once they had lost more than 25% of their body weight or had problems with ambulating, feeding, or grooming.

The replication of VSV-ΔM51-GFP in tumor tissues

To evaluate the kinetics of viral replication within the prostate tumor lesions using sets of VSV-ΔM51-GFP for treatment of prostate cancer, animals were killed at various time points after localized injections of VSV-ΔM51-GFP. Tissue samples were obtained and subjected to

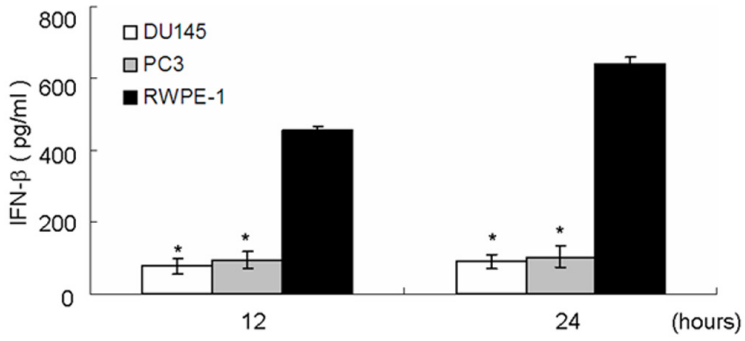

Figure 2. Human prostate carcinoma cells (DU145, PC3) and human prostatic epithelial cell lines (RWPE-1) were infected with VSV-ΔM51-GFP. Culture media were assayed by ELISA to detect human IFN-β production at 12 h and 24 h post-infection. (The symbol *represents P < 0.05 compared with RWPE-1).

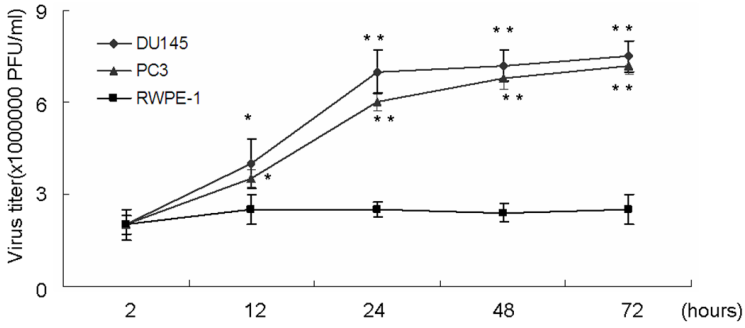

Figure 3. DU145; PC3 and RWPE-1 cells were inoculated at MOIs of 0.1 with VSV-ΔM51-GFP for 1 h as indicated and cultured for 2, 12, 24, and 48 h. At several time points post-infection, the virus titer in the culture medium was determined by plaque assays in VERO cells. The results are represented as the means ± SDs of 3 separate experiments. (The symbol *represents P < 0.05 compared with RWPE-1, the symbol **represents P < 0.01 compared with RWPE-1).

plaque assays to determine the viral yield as described as above [22]. In a separate experiment, a group of tumor-bearing animals that had been injected with the RPMI-1640 control was followed for survival, which was scored daily in all animals. Tissue samples were homogenized in 0.5 mL of PBS, and serial dilutions were applied to confluent Vero cells for 45 min. Subsequently, plates were overlaid with 0.5% agarose in medium and plaques were grown for 12, 24, and 48 h. Plaques were counted by visual inspection.

Immunohistochemical and HE staining of tissue

Five-micrometer sections were prepared from paraffin-embedded tissues, and tissues were extracted from paraffin as described previously [19]. The tissues were stained with a primary antibody against VSV-G (Sigma, USA) following the protocol as described previously [23].

Statistical analysis

The non-parametric one-way analysis of variance (ANOVA) with Dunnett's post-hoc analysis was performed to compare and analyze statistical differences using SPSS 17.0 software. The data are expressed as the mean ± SD of at least three separate experiments. A *P* value less than 0.05 (P < 0.05) was considered to be statistically significant for the differences and is denoted with an asterisk in the corresponding figures.

Results

The cytotoxicity of VSV-ΔM51-GFP against prostate tumor cells and normal prostate epithelial cells in vitro

The effect of VSV-ΔM51-GFP infection on the growth and viability of prostate cancer cells was evaluated. The DU145 and RWPE-1 cell lines were treated with different MOIs of the virus (0.01 and 0.1) for 48 hours, and the viability of infected and control cells was measured using an MTT assay. As shown in **Figure 1B**, VSV-ΔM51-GFP infection resulted in a considerable decrease in the percentage of viable DU145 cells and PC3 cells. The results indicated that VSV-ΔM51-GFP inhibited the viability of Du145 cells and PC3 cells in a dose and time dependent manner. At the MOI of 0.1, The cytotoxic effect of VSV-ΔM51-GFP was > 85% in the Du145 cell line, > 70% in the PC3 cell line, < 20% in the RWPE-1 cells, and < 5% in the RPMI-1640 negative control cells. At the MOI of 0.01, the mortality of DU145 cells was approximately 42-45%, the mortality of PC3 cells was approximately 36-41%, compared to < 15% in the RWPE-1 cells, and < 3% in the RPMI-1640 negative control group. These in vitro results show

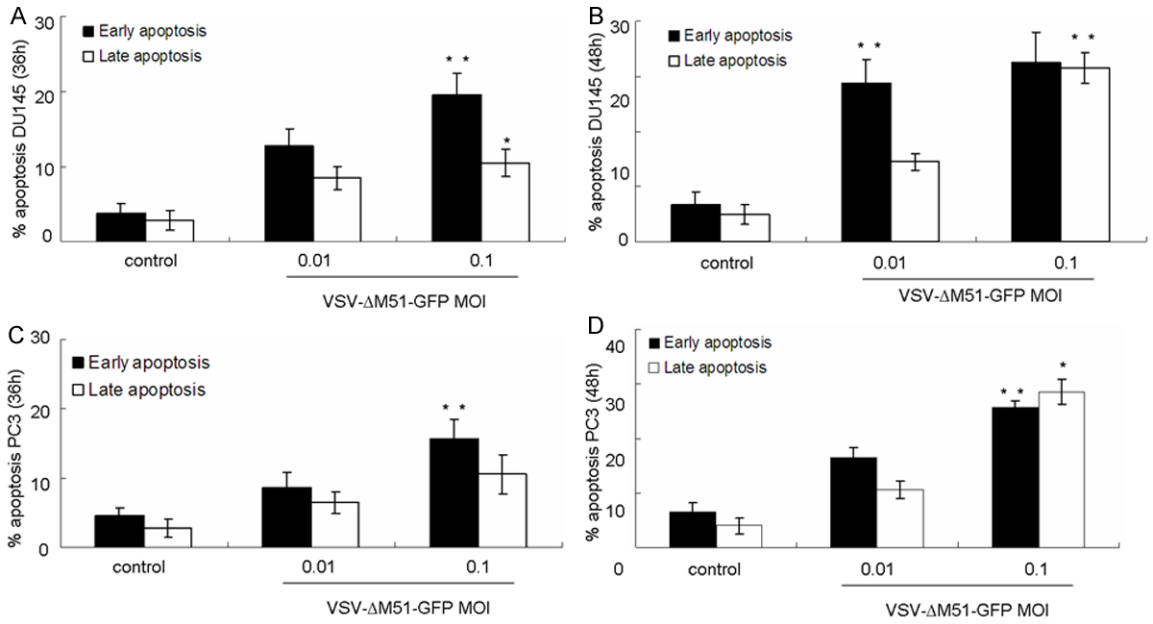

Figure 4. The Effect of VSV-ΔM51-GFP on the Induction of Apoptosis in Cancer Cell Line, DU145 cells and PC3 cells were infected with different concentrations of VSV-ΔM51-GFP (MOI of 0.01 and 0.1) for 36 and 48 hours. Annexin-V and PI staining methods were employed for detection of apoptosis using flow cytometry. The percentages of early and late apoptotic cells were increased following exposure to VSV-ΔM51-GFP in a concentration and time-dependent manner. The results (Mean ± SD) represent at least 3 separate experiments. Differences between VSV-M51-GFP infected and non-infected cells were statistically analyzed by ANOVA (The symbol *represents $P < 0.05$, the symbol **represents $P < 0.01$).

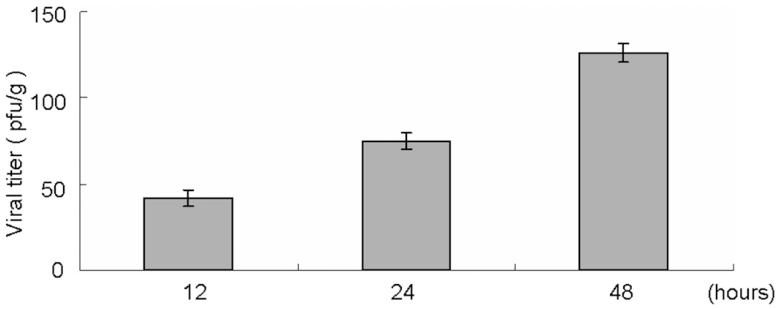

Figure 5. Replication ability of VSV-ΔM51-GFP and tissue distribution of replication-competent virus. Mice were injected with 10^7 PFU VSV-ΔM51-GFP. The mice were sacrificed at time points of 12, 24, and 48 h after viral inoculation. The tumor tissues were frozen and virus titers were determined by plaque assays. The results are presented as the mean pfu/g ± SEM (n = 3). pfu, plaque-forming unit; VSV, vesicular stomatitis virus.

that VSV-ΔM51-GFP shows good preferential oncolytic effect in tumor cells and has a high toxicity rate, while normal cells are relatively safe from VSV-ΔM51-GFP.

VSV is very sensitive to IFN [30]. To determine the status of the IFN-beta response, DU145, RWPE-1, PC3 cells were infected with 0.1 pfu of VSV-ΔM51-GFP for 12 and 24 h (**Figure 2**). The concentration of IFN-beta is low in the DU145 and PC3 cells, whereas the concentration of IFN-beta is high in the RWPE-1 cells. The selectivity of VSV-ΔM51-GFP replication in DU145 and PC3 prostate cancer cells is believed to be due to a defect in IFN-beta signaling in tumor cells compared to normal cells. The DU145 cells and PC3 may not have the IFN-beta signal interference. IFN-beta led to increased cell viability in the RWPE-1 cells. This showed that VSV-ΔM51-GFP is highly sensitive to the IFN response in normal prostate epithelial cells.

VSV-ΔM51-GFP replication in the prostate cancer cell line (DU145, PC3) and the normal human prostate epithelial cell line RWPE-1

There is a cell-specific difference in the kinetics and efficiency of virus release that is related to

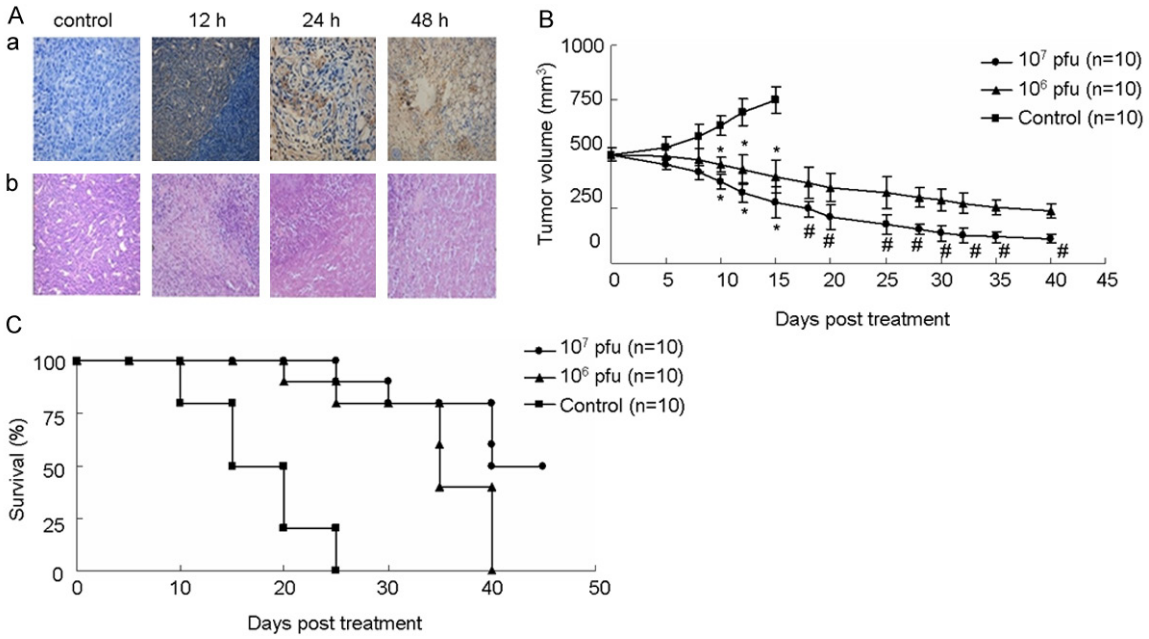

Figure 6. (A) Each mouse was injected with 10^7 PFU VSV-ΔM51-GFP. Mice were euthanized at 12, 24, and 48 h after viral injection. Paraffin-embedded prostate tissues were stained with HE (a), and the presence of VSV-ΔM51-GFP was established by immunohistochemical staining of prostate from TRAMP using an anti-VSV antibody (b). Representative slides were prepared and visualized at 20 × magnification. The results were scored by a pathologist (n = 3). TRAMP, transgenic adenocarcinoma of the mouse prostate; VSV, vesicular stomatitis virus. (B) Efficacy of VSV-ΔM51-GFP in nude mice bearing human prostate tumors. Four- to six-week-old male athymic nude mice were subcutaneously injected with DU145 cells in the right flank. Tumors were established by day 14, and the mice were randomly divided into three groups (n = 10 per group). One group served as a control and received one i.t. administration of 100 μl of RWPI-1640 only. The other two groups were treated i.t. once with VSV-ΔM51-GFP at a dose of 1×10^7 PFU or 1×10^6 PFU in 100 μl volume. The tumor size was monitored by caliper measurements, and tumor volume was calculated according to the following formula: grams = (length in centimeters × width^2)/2. The groups were compared using two-way ANOVA, followed by the Bonferroni post-test for multiple comparisons (The symbol *represents $P < 0.05$ compared with control, the symbol #represents $P < 0.05$ compared with 10^6 pfu). (C) Prostate tumors were established as described above, and mice received VSV-ΔM51-GFP by intratumoral injection every day (three doses total). Mice treated with either 10^6 PFU or 10^7 PFU were protected and the tumor was significantly inhibited, prolonging the survival of the animal.

the type of tumor cell line studied [24]. Therefore, we aimed first to check the ability of DU145 cell line and PC3 cell line to support the replication of VSV-ΔM51-GFP. Measurement of the virus release into the supernatant showed that DU145 cells and PC3 cells appeared to lag at the 2 h point, but by 12, 24, 48 and 72 h, the titer of released virus was high at the indicated MOI of 0.1 (**Figure 3**). These results show that VSV-ΔM51-GFP is increasingly replicating in DU145 and PC3 prostate cancer cells. In contrast, the replication of VSV-ΔM51-GFP was low in the RWPE-1 cells; at 2 hours after injection, the initial level of virus was observed in the prostate cells (approximately 2×10^6 PFU/ml). The highest titer of VSV-ΔM51-GFP was approximately 7.5×10^6 PFU/ml in DU145 cells and 7.2×10^6 PFU/ml in PC3 cells. These data are shown in **Figure 3**. VSV-ΔM51-GFP replication in DU145 cells and PC3 cells are much greater than in RWPE-1 cells, indicating that VSV-ΔM51-GFP is relatively safe.

VSV-ΔM51-GFP induce apoptosis in DU145 and PC3 prostate cancer cells

To ascertain whether or not the inhibitory effect of VSV-ΔM51-GFP on DU145 cells and PC3 cells was associated with the induction of apoptosis, Annexin-V and PI double staining were performed and analyzed using flow cytometry. According to the method, early apoptotic cells are characterized as Annexin-Vpositive and PI-positive. Subsequently, controls are considered as annexin-negative and PI-negative cells. DU145 cells and PC3 cells were infected with MOI of 0.01 and 0.1 of VSV-ΔM51-GFP for

36 hours and 48 hours and analyzed by flow cytometry. The results indicated that an increase in the rate of early (P = 0.0089) and late (P = 0.037) apoptotic cells were detected in DU145 cells following infection by MOI of 0.1 of VSV-ΔM51-GFP in 36 hours (**Figure 4A**). DU145 Cells infected by MOI of 0.01 of the virus revealed a significant increase of early apoptotic cells after 48 hours (**Figure 4B**). A remarkable elevation in the percentage of late apoptotic cells were also observed at the MOI of 0.1 of virus after 48 hours (P = 0.0057) (**Figure 4B**). PC3 Cells infected by MOI of 0.1 of the virus revealed a significant increase of early apoptotic cells after 36 hours (**Figure 4C**). A remarkable elevation in the percentage of early and late apoptotic cells were also observed at the MOI of 0.1 of virus after 48 hours (P = 0.0077, P = 0.031) (**Figure 4D**). Our data demonstrated that infection of DU145 cells and PC3 cells by increasing concentrations of VSV-ΔM51-GFP was accompanied by a notable shift of the viable cells to the apoptotic cells in a time and dose-dependent manner.

Presence of live virus in prostatic tissue of the nude mice

To determine whether the in vitro experimental data correlated with the presence of infectious virus, at 12 to 48 hours after injection, the nude mice were sacrificed their xenografts were harvested and frozen. Homogenized tissues were titrated by plaque assays to quantify viral delivery and replication within various tissues. At 12 hours after VSV-M51-GFP injection in nude mice (**Figure 5**), the viral titer was 42.0 ± 4.7 pfu/g; at 24 hours after injection, the viral titer was 75.0 ± 4.5 pfu/g; and at 48 hours after injection, the viral titer was 126.0 ± 5.6 pfu/g, suggesting that VSV-ΔM51-GFP was readily infected or able to replicate rapidly in vitro.

Effect VSV-ΔM51-GFP of on human prostate cancer tumors in vivo

To test the efficacy of VSV-ΔM51-GFP in vivo and to determine the relevance of our in vitro results to an in vivo situation, we chose DU145 cell lines for in vivo testing based on our in vitro virus permissiveness and oncolysis experiments. DU145 cells are highly permissive to VSV-ΔM51-GFP. DU145 were injected subcutaneously into the right flank of male nude mice (n = 30). Once the mice developed palpable tumors (about 10 mm), they were divided into three equal groups (n = 10 for each group). A control group received an intratumoral (i.t.) injection of 100 μl RPMI-1640, one group received an i.t. injection of VSV-ΔM51-GFP at a dose of 1×10^7 pfu in 100 μl volume and one group received an i.t. injection of VSV-ΔM51-GFP at a dose of 1×10^6 pfu in 100 μl volume. The mice were monitored daily for signs of distress, and tumor size was measured every other day for 40 days. At a dose of 1×10^7 pfu in 100 μl had the greatest therapeutic effect in mice bearing prostate tumors (**Figure 6B**). VSV-ΔM51-GFP seemed to stabilize tumor growth compared to the treatment of tumors with RPMI-1640, which had no effect on tumor growth.

Figure 6C shows the survival plots of nude mice seeded with prostate tumors and then treated with an intratumoral injection with RPMI-1640, 10^6 PFU or 10^7 PFU VSV-ΔM51-GFP. These treatments were well tolerated by the nude mice; the mean time to death (MTD) with no mortalities in the RPMI-1640-treated mice was approximately 15 days. However, mice treated with either 10^6 PFU or 10^7 PFU were protected and the tumor was significantly inhibited, prolonging the survival of the animal. This experiment demonstrates the remarkable ability of VSV-ΔM51-GFP to produce durable cures in an aggressive, disseminated prostate tumor model.

Discussion

Taxane chemotherapeutic agents, such as docetaxel, are the main forms of treatment for metastatic, castration-resistant prostate cancers [25-27]. However, due to the emergence of drug-resistant cells and drug side effects, this line of treatment is largely palliative and not curative. Therefore, to successfully relieve drug side effects and overcome prostate cancer, the development of new anti-tumor methods with specificity and lower side effects is a very urgent task.

Although oncolytic herpes, reoviruses, and adenoviruses have been previously tested in prostate cancer models [28-30]. VSV holds great promise due to its distinct targeting approach, high inherent infection efficiency, and proven track record of broad spectrum oncolytic activ-

ity without requiring the application of transduction enhancement agents [22]. To show that VSV-ΔM51-GFP was able to infect human and mouse prostate cell lines, we utilized three cell lines representing normal prostate epithelial cells (RWPE-1) and human prostate cancer cells (DU145, PC3) as shown in **Figure 1A** and **1B**. To evaluate the relative efficacy of VSV-ΔM51-GFP as an OV, we initially compared different doses of VSV-ΔM51-GFP. There was a direct correlation between an increased viral titer and decreased cell survival in the Du145 cell line and PC3 cell line compared with non-neoplastic control cells. The RWPE-1 cells were less effectively killed by VSV-ΔM51-GFP, but VSV-ΔM51-GFP had a strong effect against Du145 cells and PC3 cells, indicating that VSV-ΔM51-GFP is able to infect and lyse cancer cells while sparing nonmalignant cells. While there is still damage to normal cells, these data showed that VSV-ΔM51-GFP is the limitation in therapeutic applications, as we know one of the biggest problems in viral cancer treatments is about its safety. It was reported that when animals were injected with high dose of VSV-wt, neurotoxicity, such as hind limb paralysis occurred, However, VSV-ΔM51-GFP have been generated that are not neurotropic but retain their oncolytic activity. A considerable promotion in the knowledge of oncolytic viruses and their emergence to trigger apoptosis cascades has led many research groups to characterize the possible roles of such viruses in different types of malignancies [31, 32]. Oncolytic viruses have been contributed to induce apoptosis in cancer cells and emerged as novel and promising anti-cancer agents [33]. It has been demonstrated that VSV-wt induces apoptosis via the mitochondrial pathway due to wt M protein inhibition of gene expression, while VSV-ΔM51-GFP, with a pathway [34]. With the incidence of prostate cancer mutant M protein, induces apoptosis primarily via the death receptor increased year by year, lack of effective treatment, and better-tolerated anti-cancer approaches [35] motivated us to elucidate the possible role of VSV-ΔM51-GFP in growth regulation of prostate cancer cells. We designed our experiments to characterize the effect of VSV-ΔM51-GFP on the regulation of cell growth and induction of apoptosis in prostate cancer cell line (DU145, PC3).

VSV-ΔM51-GFP is an oncolytic virus that can infect and kill cells that have defects in their cellular antiviral immunity, such as the IFN response pathway. It has been reported that 80% of tumor cells are defective in type I IFN signaling [28-30]. Our data suggest that due to a defect in the IFN response (**Figure 2**), there was no change in the death of prostate cancer cells (DU145, PC3), and the pretreatment of RWPE-1 normal prostate epithelial cells with IFN led to an increase in cell survival.

Intratumoral injection is a feasible method to treat human prostate cancer. One advantage of intratumoral injection is that local administration would ensure maximal uptake of virus by tumor cells. In vitro, it has been demonstrated that an intraprostatic tumor VSV-ΔM51-GFP injection enables viral replication and amplification sufficient to inhibit growing tumors (**Figures 5** and **6B**), as shown in **Figure 6B** and **6C**, we can also conclude that 10^7 PFU of VSV-ΔM51-GFP can inhibit the growth of tumor more effectively than 10^6 PFU VSV-ΔM51-GFP and that VSV-ΔM51-GFP significantly prolonged the survival time of nude mice. These results suggest that VSV-ΔM51-GFP inhibited the growth of the tumor volume in a dose- and time-dependent manner. VSV-ΔM51-GFP can make the tumor shrink, but it still cannot make the tumor disappear. One reason for this is that the neutralizing humoral immune response generated by VSV-ΔM51-GFP exposure will likely reduce the efficacy of an injection by blunting the ability of progeny viruses to be generated, thus reducing the opportunity for a sustained infection in immunocompetent hosts. Another reason for this is that the viruses cannot spread effectively in the tumor tissue because of the complex tumor microenvironment and compromised immune responses. Recently, research has suggested the efficacy of viral oncolysis has improved with the combination of virotherapy and chemotherapeutic drugs [36-39]. In the future, we will examine the combination of VSV-ΔM51-GFP and chemotherapeutic drugs to improve the oncolytic effects.

Conclusions

These findings provide evidence that vesicular stomatitis virus is a possible therapeutic OV for prostate cancer treatment, and we have found that VSV-ΔM51-GFP enables viral replication and amplification sufficiently to selectively kill cancer cells while sparing normal cells. The primary mechanism for cell death is apparently

oncolysis due to a defective IFN response. The observed inhibition of cell growth was associated with the induction of apoptosis, and was notably under the control of virus replication. These results suggest that control of locally advanced prostate cancer in humans [40] may be achievable through injection of a safe oncolytic virus and provides a new approach for the treatment of prostate cancer.

Acknowledgements

This work was supported by the Shanghai Education Commission Research and Innovation projects (No. 12ZZ034).

Disclosure of conflict of interest

None.

Address correspondence to: Dr. Denglong Wu, Department of Urology, Tongji Hospital of Tongji University, 389 Xincun Road, Shanghai 200065, China. Tel: 86-021-66111532; Fax: 86-021-66111533; E-mail: wudenglongtj@163.com

References

[1] Mitchell RE, Chang SS. Current controversies in the treatment of high-risk prostate cancer. Curr Opin Urol 2008; 18:263-268.

[2] Sia M, Rosewall T, Warde P. Radiotherapy as primary treatment modality. Front Radiat Ther Oncol 2008; 41: 15-25.

[3] Moore CM, Pendse D, Emberton M. Photodynamic therapy for prostate cancer-a review of current status and future promise. Nat Clin Pract Urol 2009; 6: 18-30.

[4] Albertsen PC, Hanley JA, Fine J. 20-year outcomes following conservative management of clinically localized prostate cancer. JAMA 2005; 293: 2095-2101.

[5] Yang C, Qi GS, Rong RM, He J. Clinical features and treatment strategies for older prostate cancer patients with bone metastasis. Asian J Androl 2013; 15: 759-763.

[6] So A, Gleave M, Hurtado-Col A, Nelson C. Mechanisms of the development of androgen independence in prostate cancer. World J Urol 2005; 23: 1-9.

[7] Ahmed M, Puckett S, Lyles DS. Susceptibility of breast cancer cells to an oncolytic matrix (M) protein mutant of vesicular stomatitis virus. Cancer Gene Ther 2010; 17: 883-892.

[8] Li XQ, Ke XZ, Wang YM. Treatment of Malignant Melanoma by Downregulation of XIAP and Overexpression of TRAIL with a Conditionally Replicating Oncolytic Adenovirus. Asian Pac J Cancer Prev 2012; 13: 1471-1476.

[9] Galivo F, Diaz RM, Thanarajasingam U, Jevremovic D, Wongthida P, Thompson J, Kottke T, Barber GN, Melcher A, Vile RG. Interference of CD40L-mediated tumor immunotherapy by oncolytic VSV. Hum Gene Ther 2010; 21: 439-450,

[10] Edge RE, Falls TJ, Brown CW, Lichty BD, Atkins H, Bell JC. A let-7 MicroRNA-sensitive vesicular stomatitis virus demonstrates tumor-specific replication. Mol Ther 2008; 16: 1437-1443.

[11] Huang TG, Ebert O, Shinozaki K, Garcia-Sastre A, Woo SL. Oncolysis of hepatic metastasis of colorectal cancer by recombinant vesicular stomatitis virus in immune-competent mice. Mol Ther 2003; 8: 434-440.

[12] Ahmed M, Puckett S, Lyles DS. Susceptibility of breast cancer cells to an oncolytic matrix (M) protein mutant of vesicular stomatitis virus. Cancer Gene Ther 2010; 17: 883-892.

[13] Wei N, Fan JK, Gu JF, He LF, Tang WH, Cao X, Liu XY. A double-regulated oncolytic adenovirus with improved safety for adenocarcinoma therapy. Biochem Biophys Res Commun 2009; 388: 234-239.

[14] Altomonte J, Wu L, Meseck M, Chen L, Ebert O, Garcia-Sastre A, Fallon J, Mandeli J, Woo SL. Enhanced oncolytic potency of vesicular stomatitis virus through vector-mediated inhibition of NK and NKT cells. Cancer Gene Ther 2009; 16: 266-278.

[15] Ausubel LJ, Meseck M, Derecho I, Lopez P, Knoblauch C, McMahon R, Anderson J, Dunphy N, Quezada V, Khan R, Huang P, Dang W, Luo M, Hsu D, Woo SL, Couture L. Current good manufacturing practice production of an oncolytic recombinant vesicular stomatitis viral vector for cancer treatment. Hum Gene Ther 2011; 22: 489-497.

[16] Wollmann G, Tattersall P, van den Pol AN. Targeting human glioblastoma cells: comparison of nine viruses with oncolytic potential. J Virol 2005; 79: 6005-6022.

[17] Breitbach CJ, Paterson JM, Lemay CG, Falls TJ, McGuire A, Parato KA, Stojdl DF, Daneshmand M, Speth K, Kirn D, McCart JA, Atkins H, Bell JC. Targeted inflammation during oncolytic virus therapy severely compromises tumor blood flow. Mol Ther 2007; 15: 1686-1693.

[18] Quiroz E, Moreno N, Peralta PH, Tesh RB. A human case of encephalitis associated with vesicular stomatitis virus (Indiana serotype) infection. Am J Trop Med Hyg 1988; 39: 312-314.

[19] Ahmed M, Marino TR, Puckett S, Kock ND, Lyles DS. Immune response in the absence of neurovirulence in mice infected with M protein mutant vesicular stomatitis virus. J Virol 2008; 82: 9273-9277.

[20] Kelly EJ, Nace R, Barber GN, Russell SJ. Attenuation of vesicular stomatitis virus encephalitis through microRNA targeting. J Virol 2010; 84: 1550-1562.
[21] 21. Wollmann G, Rogulin V, Simon I, Rose JK, van den Pol AN. Some attenuated variants of vesicular stomatitis virus show enhanced oncolytic activity against human glioblastoma cells relative to normal brain cells. J Virol 2010; 84: 1563-1573.
[22] Hadaschik BA, Zhang K, So AI, Fazli L, Jia W, Bell JC, Gleave ME, Rennie PS. Oncolytic vesicular stomatitis viruses are potent agents for intravesical treatment of high-risk bladder cancer. Cancer Res 2008; 68: 4506-4510.
[23] Thirukkumaran CM, Nodwell MJ, Hirasawa K, Shi ZQ, Diaz R, Luider J, Johnston RN, Forsyth PA, Magliocco AM, Lee P, Nishikawa S, Donnelly B, Coffey M, Trpkov K, Fonseca K, Spurrell J, Morris DG. Oncolytic Viral Therapy for Prostate Cancer: Efficacy of Reovirus as a Biological Therapeutic. Cancer Res 2010; 70: 2435-2444.
[24] Yap TA, Zivi A, Omlin A, de Bono JS. The changing therapeutic landscape of castration-resistant prostate cancer. Nat Rev Clin Oncol 2011; 8: 597-610.
[25] Yu DC, Sakamoto GT, Henderson DR. Identification of the transcriptional regulatory sequences of human kallikrein 2 and their use in the construction of calydon virus 764, an attenuated replication competent adenovirus for prostate cancer therapy. Cancer Res 1999; 59: 1498-1504.
[26] Thirukkumaran CM, Nodwell MJ, Hirasawa K, Shi ZQ, Diaz R, Luider J, Johnston RN, Forsyth PA, Magliocco AM, Lee P, Nishikawa S, Donnelly B, Coffey M, Trpkov K, Fonseca K, Spurrell J, Morris DG. Oncolytic Viral Therapy for Prostate Cancer: Efficacy of Reovirus as a Biological Therapeutic. Cancer Res 2010; 70: 2435-2444.
[27] Lee CY, Bu LX, DeBenedetti A, Williams BJ, Rennie PS, Jia WW. Transcriptional and Translational Dual-regulated Oncolytic Herpes Simplex Virus Type 1 for Targeting Prostate Tumors. Mol Ther 2010; 18: 929-935.
[28] Nguyên TL, Abdelbary H, Arguello M, Breitbach C, Leveille S, Diallo JS, Yasmeen A, Bismar TA, Kirn D, Falls T, Snoulten VE, Vanderhyden BC, Werier J, Atkins H, Vähä-Koskela MJ, Stojdl DF, Bell JC, Hiscott J. Chemical targeting of the innate antiviral response by histone deacetylase inhibitors renders refractory cancers sensitive to viral oncolysis. Proc Natl Acad Sci U S A 2008; 105: 14981-14986.
[29] Stojdl DF, Lichty B, Knowles S, Marius R, Atkins H, Sonenberg N, Bell JC. Exploiting tumor-specific defects in the interferon pathway with a previously unknown oncolytic virus. Nat Med 2000; 6: 821-825.
[30] Stojdl DF, Lichty BD, tenOever BR, Paterson JM, Power AT, Knowles S, Marius R, Reynard J, Poliquin L, Atkins H, Brown EG, Durbin RK, Durbin JE, Hiscott J, Bell JC. VSV strains with defects in their ability to shutdown innate immunity are potent systemic anticancer agents. Cancer Cell 2003; 4: 263-275.
[31] Cripe TP, Wang PY, Marcato P, Mahller YY, Lee PW. Targeting cancer-initiating cells with oncolytic viruses. Mol Ther 2009; 17: 1677-1682.
[32] Kasibhatla S, Tseng B. Why target apoptosis in cancer treatment? Mol Cancer Ther 2003; 2: 573-580.
[33] Guse K, Cerullo V, Hemminki A. Oncolytic vaccinia virus for the treatment of cancer. Expert Opin Biol Ther 2011; 11: 595-608.
[34] Gaddy DF, Lyles DS. Vesicular stomatitis viruses expressing wildtype or mutant M proteins activate apoptosis through distinct pathways. J Virol 2005; 79: 4170-4179.
[35] Svajdler M, Rychly B, Benicky M. Targeted therapy of melanoma: fact or fiction. Cesk Patol 2011; 47: 165-167.
[36] Kambara H, Saeki Y, Chiocca EA. Cyclophosphamide allows for in vivo dose reduction of a potent oncolytic virus. Cancer Res 2005; 65: 11255-11258.
[37] Thomas MA, Spencer JF, Toth K, Sagartz JE, Phillips NJ, Wold WS. Immunosuppression enhances oncolytic adenovirus replication and antitumor efficacy in the Syrian hamster model. Mol Ther 2008; 16: 1665-1673.
[38] Ungerechts G, Springfeld C, Frenzke ME, Lampe J, Parker WB, Sorscher EJ, Cattaneo R. An immunocompetent murine model for oncolysis with an armed and targeted measles virus. Mol Ther 2007; 15: 1991-1997.
[39] Qiao J, Wang H, Kottke T, White C, Twigger K, Diaz RM, Thompson J, Selby P, de Bono J, Melcher A, Pandha H, Coffey M, Vile R, Harrington K. Cyclophosphamide facilitates antitumor efficacy against subcutaneous tumors following intravenous delivery of reovirus. Clin Cancer Res 2008; 14: 259-269.
[40] Shelley MD, Kumar S, Wilt T, Staffurth J, Coles B, Mason MD. A systematic review and meta-analysis of randomised trials of neoadjuvant hormone therapy for localised and locally advanced prostate carcinoma. Cancer Treat Rev 2009; 35: 9-17.